A NOVEL MPPT CONTROLLED GRID-CONNECTED PHOTOVOLTAIC SYSTEM WITH DUAL FUNCTIONALITY OF ACTIVE POWER INJECTION AND REACTIVE POWER COMPENSATION IN A SINGLE PHASE SYSTEM

Anant NAIK , Udaykumar YARAGATTI

Department of Electrical and Electronics Engineering, National Institute of Technology Karnataka, Surathkal Srinivasnagar, Mangalore, Karnataka, INDIA - 575 250 Phone:+91-824-2474823 Ext.:3453, Fax:+91-824-2474033
Email: ajn@gec.ac.in

Abstract: *This paper deals with the study of integration of distributed generation with active power filtering functionality in a single- phase system. Here the active power generated by the photovoltaic (PV) system is injected into the grid system through a coupling capacitor whenever solar input is available and the remaining capacity of the power conditioning inverter is used to compensate for the reactive power demand. The control algorithm used in this paper is simple and easy to implement. The PV system is integrated through a novel and simple MPPT technique. The system is simulated and analyzed for a given non-liner load with and without renewable source at different atmospheric conditions using MATLAB/Simulink tool. The grid current becomes sinusoidal and in phase with the grid voltage and hence the source current THD is reduced to great extent.*

Key words*: active power filter, photovoltaic, maximum power point tracking, current controlled voltage source inverter.*

1. Introduction

Grid – connected renewable power is the main path through which the energy fuel mix can be brought in line with the set goal of reducing carbon emissions. The distributed generation (DG) concept is becoming more and more popular as it can provide more reliability, reduced emissions and provide additional power quality benefits [1]. Solar energy, being abundant and widespread in its availability, is one of the attractive sources of energy. Unfortunately, PV generation system suffers from disadvantages such as poor conversion efficiency and nonlinear I-V characteristics. Hence it is required to extract maximum available power from the PV array. Several maximum power point tracking (MPPT) algorithms are reported in the literature [2]-[5]. When operated in grid connected mode the inverter is current controlled as the voltage at the point of common coupling (PCC) is imposed by the grid. Here the PV system injects only the active power to the grid through inverter and the reference current is computed from active power that PV system generates at a given time [6]. Several single-phase, single-stage grid interactive inverter topologies have been proposed [7], [8].

In the past few years, there has been considerable advancement in the field of power semiconductor technology. The intensive use of these devices in various applications has led to serious power quality issues. The regulatory commissions have specified acceptable harmonic levels that are allowed into the grid. To solve the power quality problems, active power filters (APF) are extensively used. Many APF topologies and control algorithms are reported in the literature [9]. The use of APF requires an additional cost. It is possible to integrate power quality functions by compensating the reactive power and the current harmonics drawn by the local non linear load into the grid - connected PV system just by modifying the control strategy to incorporate APF features [10].

In this paper, a single-phase, grid-interactive PV system with novel MPPT algorithm is proposed. The idea is to integrate PV system with shunt APF capabilities. Here the PV array is connected to the grid system with its inverter performing the additional function of APF besides real power injection. This is achieved with suitable modifications in the control algorithm without any additional hardware or power circuit for making the existing inverter to act as APF too. Hence the overall cost of the system is reduced. The single-

phase, grid interactive PV system along with its MPPT algorithm is modeled and simulated in MATLAB/Simulink environment. The results show that this PV system injects active power at the PCC and compensates for load reactive power. Hence the source/grid power factor is improved.

In this paper, section 2 describes the overall system description. Detailed PV system modeling with new MPPT method is explained in section 3. The control theory and the system modeling are covered in section 4 and 5 respectively. Section 6 covers design aspects of APF. The results and discussion are given in section 7 and conclusion is presented in section 8.

2. System Description

The system being studied is shown in figure1. It consists of a current controlled voltage source inverter (CC-VSI) fed from a PV source. It feds current into the grid and the local load through a series connected filter inductance L_c. The output DC voltage of PV cell is maintained constant by capacitor C_{dc} at the input of the inverter as the power output of the inverter oscillates at twice the line frequency. Also it is require to connect a smoothing reactor in series with the local load to suppress the load current spikes.

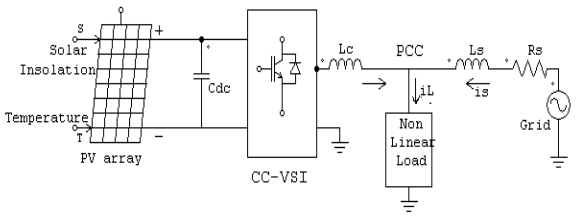

Fig. 1. Grid connected PV system

3.PV Modeling and its Characteristics

The electrical output from the PV cell is described by the I-V characteristics. These I-V characteristics of solar cell can be obtained by drawing an equivalent circuit of the device as shown in the figure (2)[11], [12].

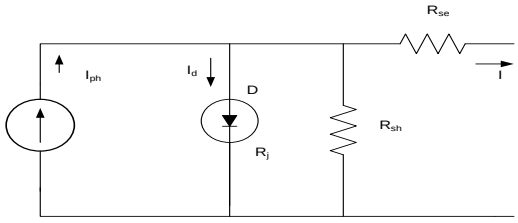

Fig. 2. Equivalent circuit of PV module.

The generation of current I_{ph} by light is represented by a current generator in parallel with a diode which represents the p-n junction. The output current I_c is then equal to the difference between the light generated current I_{ph} and the diode current I_d. In practical applications, solar cells do not operate under standard conditions. The two most important effects that must be allowed for are due to the variable temperature and irradiance. The three most important electrical characteristics of a module are the short circuit current, open circuit voltage and the maximum power point as function of temperature and irradiance. To simulate PV array, the mathematical model neglecting shunt resistance R_{sh} is used according to the following set of equations:

The output voltage of PV cell is a function of photo current and it depends upon solar insolation level.

$$V_c = \frac{AkT_c}{e}\ln\left(\frac{I_{ph}+I_d-I_c}{I_d}\right) - R_{se}I_c \qquad (1)$$

where, I_c and V_c are cell output current and voltage, respectively; I_d is the reverse saturation current of the diode; T_c is the cell temperature at standard test conditions (STC) in ^{0}C; k is Boltzmann's constant in J/^{0}C; e is electronic charge; I_{ph} is the light-generated current; A=1.92 is ideality factor; R_{se} is the series resistance. The array voltage is obtained by multiplying equation (1) by the number of the cells connected in series, N_s. The array current is obtained by multiplying the cell current by the number of the cells connected in parallel, N_p. This value of current is valid for a certain cell operating temperature T_c and its corresponding solar insolation level S_c. A method to include the effects of the changes in temperature and solar insolation levels is given in [13]. According to this, a model is obtained for known temperature (T_c) and solar insolation (S_c). The solar cell operating temperature varies as a function of solar insolation level and ambient temperature. The cell output voltage and cell photocurrent are affected by ambient temperature. These effects are represented by temperature coefficients C_{TV} and C_{TI} for cell output voltage and cell photocurrent respectively.

$$C_{TV} = 1+\beta_T(T_a - T_x) \qquad (2)$$

$$C_{TI} = 1+\frac{\gamma_T}{S_c}(T_x - T_a) \qquad (3)$$

where T_a and S_a are ambient temperature and cell solar insolation level at STC, respectively. T_x is any other temperature. β_T and Υ_T are constants specified by the manufacturers. Similarly, the change in solar insolation level causes a change in the cell photocurrent and operating temperature. Therefore, the change in the cell output voltage and the cell photocurrent are corrected by the two factors,

$$C_{SV} = 1 + \beta_T \alpha_S (S_x - S_a) \quad (4)$$

$$C_{SI} = 1 + \frac{1}{S_c}(S_x - S_a) \quad (5)$$

where, S_x is the new level of solar insolation. α_s represents the slope of the change in the solar insolation level. Using correction factors given in equations (2)-(5), the new values of cell output voltage V_{cx} and photocurrent I_{phx} are given for any temperature T_x and solar insolation S_x as

$$V_{cx} = C_{TV} C_{SV} V_c \quad (6)$$

$$I_{phx} = C_{TI} C_{SI} I_{ph} \quad (7)$$

where, V_c and I_{ph} are the cell output voltage and photocurrent at STC, respectively.

The rating of a PV module is estimated by the maximum power at STC which corresponds to an insolation level of 1000 W/m^2 and a cell temperature of 25^{0}C. The PV cell manufacturers provide its characteristics by specifying the parameters given in table 1.
Module: Solarex MSX60, 60 W PV module at STC irradiance: 1000W/sq.m, ambient temp: 25^{0}C

Table 1. Specifications for solar array at STC

Isc	3.74 A
Voc	21 V
Pm	61.85 W
Im	3.5 A
Vm	17.1 V

Using equations (1)-(7) and the parameters at STC, the I-V and P-V characteristics of PV at different solar insolation and cell temperatures can be obtained as shown in figure (3) and figure (4).

3.1 Novel MPPT Technique

The maximum power point operation of a PV array is achieved by maximizing its output power to load. The maximum power must be determined for the changing temperature and solar irradiation

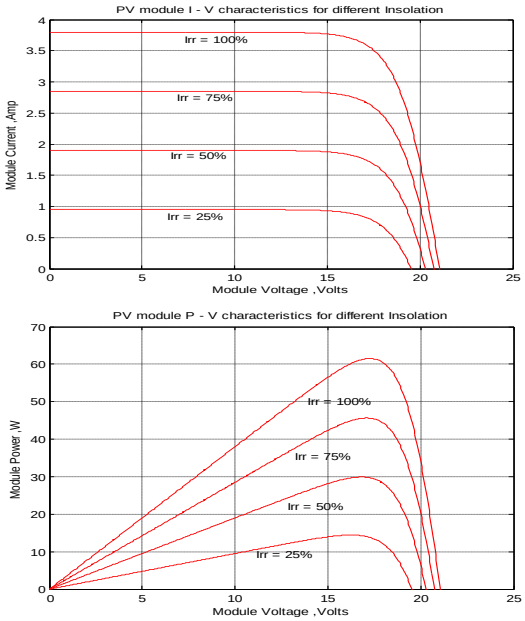

Fig. 3. The I-V and P-V characteristics at different solar insolation at 25^{0}C temperature.

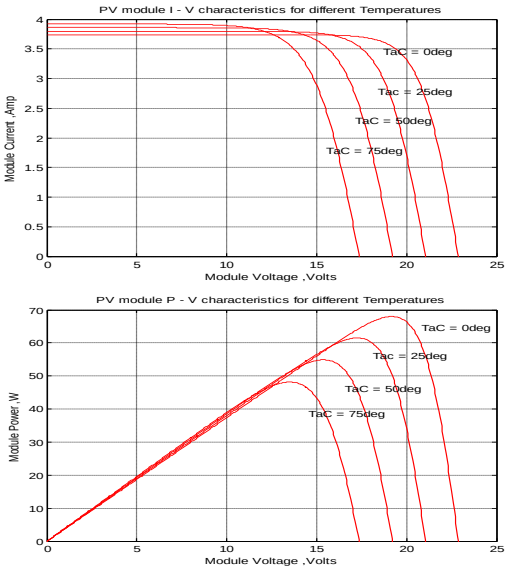

Fig. 4. The I-V and P-V characteristics at different cell temperature at 1000W/m^2 solar insolation.

level before it is compared with the operating power. The various MPPT methods used in the literature are based on the following methods [11]

1. Perturb & Observe. (P&O)
2. Incremental conductance.

Here, we propose a MPPT method based on open circuit voltage. Peak power point of the module is approximately at 76% of the module open circuit voltage. This value is fixed and does not vary much with the changes in the environmental conditions. By measuring the open circuit voltage at any given operating conditions and adjusting the module voltage to about 76% of V_{oc} the peak power can be tracked. Using equation (6), V_{oc} at any temperature and solar insolation is calculated. V_m is approximated to 0.76 times this V_{oc}. Now using equation (1), I_m and hence P_m is calculated using iterative method.

4. Control Theory

In general, we can define the PCC voltage and current as in equations (8) and (9) respectively [10].

$$v_L(t) = V_d + \sum_{k=1}^{h} V_{mk} \sin(k\omega t + \phi_{vk}) \quad (8)$$

$$i_L(t) = I_d + \sum_{k=1}^{n} I_{mk} \sin(k\omega t + \phi_{ik}) \quad (9)$$

where h and n are the highest orders of harmonics in voltage and current, respectively.
V_{mk} = peak value of the PCC voltage corresponding to the k^{th} order harmonic.
I_{mk} = peak value of the load current corresponding to the k^{th} order harmonic.
V_d = DC component present in the PCC voltage.
I_d = DC component present in the load current.
Φ_{vk} =phase angle of the PCC voltage corresponding to k^{th} order harmonics.
Φ_{ik} =phase angles of the load current corresponding to k^{th} order harmonics.

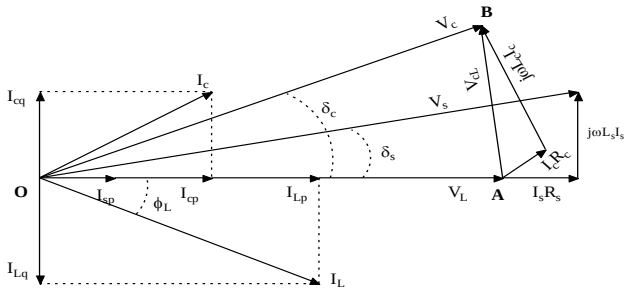

Fig. 5. Phasor diagram of the system

Figure (5) shows the phasor diagram of the proposed system of figure (1). In this figure, V_s, V_L and V_c are the rms voltages at grid, load and output of the inverter, respectively. I_s, I_L and I_c are the rms values of the currents from grid, to load and from the inverter, respectively. I_{sp}, I_{Lp} and I_{cp} are the active components while I_{sq}, I_{Lq} and I_{cq} are the reactive components of I_s, I_L and I_c respectively. The φ_L is the load power factor angle. The δ_s is the angle between V_s and V_L. δ_c is the angle between V_c and V_L. From ΔOAB in figure (5), voltage V_{cL} across the filter inductor can be given as:

$$V_{CL}^{\ 2} = V_c^{\ 2} + V_L^{\ 2} - 2V_c V_L \cos\delta_c \quad (10)$$

Now neglecting filter resistance R_c, the current through inductor I_c can be expressed as:

$$I_c \approx \frac{V_{CL}}{j\omega L_c} \quad (11)$$

Also, from inverter operation, we know that

$$V_c = m_a V_{dc} \quad (12)$$

where, m_a is the modulation index. Now using, equations (10), (11) and (12) the following equation is obtained:

$$I_c^{\ 2} = \frac{(m_a V_{dc}^{\ 2}) + V_L^{\ 2} - 2(m_a V_{dc}) V_L \cos\delta_c}{(\omega L_c)^2} \quad (13)$$

From equation (13) it is clear that the magnitude of I_c depends on $(m_a V_{dc})$ and (δ_c). For optimal control at unity power factor compensation, the active power supplied by the grid at k^{th} sampling instant should be equal to the grid apparent power $S_s(k)$. Hence

$$P_s(k) = P_{lavg}(k) + P_{sl}(k) - P_c(k) = \frac{V_{sm}(k) I_{sm}(k)}{2} \quad (14)$$

where, $P_{lavg}(k)$, $P_{sl}(k)$, $P_c(k)$ are the average load active power, output power of DC bus controller and ac side active power of the inverter at the k^{th} sampling instant, respectively.

Using equation (14), the required peak value of the grid current can be calculated as

$$I_{sm}(k) = \frac{2P_s(k)}{V_{sm}(k)} \quad (15)$$

The instantaneous grid current is obtained by multiplying the peak value by unity sine vector.

$$i_s^{\ *}(k) = I_{sm}(k) \sin(\omega k) \quad (16)$$

Further, the instantaneous grid current is compared with actual grid current (i_s) to get required compensating current, as:

$$\Delta i_s(k) = i^*_s(k) - i_s(k) \quad (17)$$

This current is given to a hysteresis comparator to generate PWM signals to drive the switches of CC-VSI.

5. System Modeling

Figure (6) shows the model of the proposed single-stage, single-phase grid interactive system. Here single-phase grid system is feeding a local non-linear load consisting of a diode rectifier bridge driving R-L load. At this load bus (PCC), a PV fed inverter is connected through filter inductor. This PV fed inverter consists of an IGBT driven H-bridge. The input DC voltage is the MPPT output voltage to this inverter.

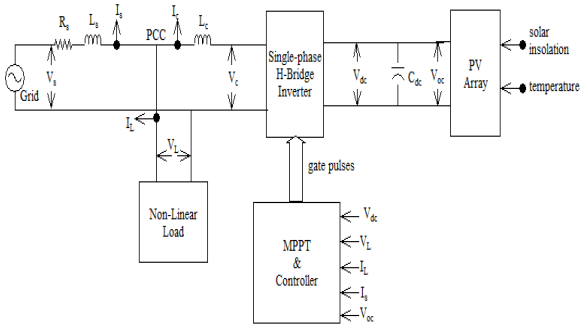

Fig.6. system model

PV array is modeled separately with different combination of solar insolation and temperature

Table 2. Simulation parameters

Location	Parameter	Value
PV	Total no of modules Maximum power generated by PV array	NsxNp=15x4=60 60x60 ≈ 3600 W
Active Power Filter	Filter resistance and inductance DC-bus capacitance	0.01Ω and 8mH 5000 μF
Grid	Grid voltage at 50 Hz	230 V
Load	Single-phase diode bridge with R-L load on its dc side.	Z=(7.5+j7.8) Ω

using equations 1-7 as explained in section III. The output voltage corresponding to the maximum power is calculated and made available by the MPPT block as described in sub section novel MPPT technique.

The overall control is carried out by the controller block and the same is shown in figure (7). Here initially average load active power is extracted using two signals v_L and i_L .The active power generated by the PV source is available at the MPPT output. The power loss in the DC-link voltage controller is to be subtracted from this PV active power. The grid active power hence is the net power required by the load minus the power available from the PV source. According to equation (15) then the peak value of source current is calculated. The unit sine wave is generated using load voltage signal and its peak value. The peak value of source current is multiplied by the unit sine vector as per equation (16). Hysteresis

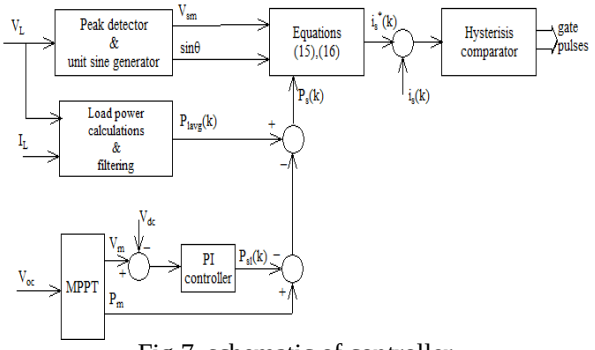

Fig.7. schematic of controller

controller is used to generate the required pulses for the CC-VSI. The error signal is generated by comparing reference current with the actual source current.

6. Design of APF power circuit

6.1 Rating of switches used in CC-VSI

The power rating of the VSI is decided by the load current THD. It lies in the range of 20-50%. In this paper we have considered a 3kVA non-linear load with current THD of 26.87%. It is operated at 230V, 50 Hz system. It means, considering a tolerance factor of 2, IGBT switches of 25A are sufficient when the PV generated power is less than the load active power. But here we have to consider maximum PV generated power of 3600W. Hence the kVA capacity of inverter is increased to 3.8

kVA. Therefore IGBT switches to be used are of rating 32A(approximately 40A).

6.2 Sizing of DC bus Capacitor

The switching frequency must be chosen high enough to cancel harmonics up to a given frequency. The design of the filter inductor L_c and the DC bus voltage V_{dc} [14] are based on (i) limiting the high frequency components of the injected currents; say 5% of the rated load current.

$$\text{Therefore, } \frac{I_{c,fs}}{I_1} = \frac{V_{c,fs}}{I_1(fs/f)\omega L_c} < 5\% \quad (18)$$

Where $I_{c,fs}$ is the rms value of the converter current at the switching frequency f_s, $V_{c,fs}$ is the rms value of the converter output voltage at the switching frequency f_s,I_1 is the rms value of the fundamental load current.

(ii) the instantaneous di/dt generated by the active filter should be greater than the di/dt of the harmonic component of the load, so that the proper harmonic cancellation can take place.

$$\text{Therefore, } V_s.\sqrt{2} + L_c\left(\frac{di}{dt}\right)_{load} < 0.5\, V_{dc} \quad (19)$$

Equations (18) and (19) allow the calculations of minimum values of L_c and V_{dc} independently. However, the selection of L_c and V_{dc} requires some sort of compromise. The converter must generate a high di/dt to cancel the harmonics. This requires small L_c. But with small L_c ,ripple increases. Similarly higher V_{dc} gives more di/dt but at the cost of the increase in the current ripple.

The capacitor is designed to limit the DC voltage ripple to a specified value, typically 1to 2%. The variation in DC voltage is given by

$$\Delta V_{dc} = (v_{dc})_{\max} - (v_{dc})_{\min} = \frac{\Delta\left[\int v_s.i_h dt\right]}{C.V_{dc}} \quad (20)$$

For h=3,5……The percentage ripple of the DC bus voltage is defined as

$$r_v = \frac{\Delta V_{dc}}{V_{dc}} \quad (21)$$

From euations (20) and (21), the capacitor value is given by

$$C = \frac{\Delta\left[\int v_s.i_h dt\right]}{r_v.V_{dc}^2} \quad (22)$$

For the given parameters of the system used in this paper the L_C and C is calculated as 8mH and 5000μF using equations (18)-(22).

7. Results and Discussions

The various parameters used for simulation are given in table 2. The operation of the system in different modes is summarized in the table 3. Figures (8), (9) and (10) show the operation of this system in different modes

Table 3. Summary of operation

case	Time interval	Mode of operation	PV power injected
I	0 - 0.1sec	Without APF and PV	0
II	0.1 - 0.2sec	APF	0
III	0.2 - 0.3sec	APF+PV	$< P_L$
IV	0.3 - 0.4sec	APF+PV	$>P_L$

Case I: Here the system operates without APF/PV power injection. From figure (8) it is clear that the source current is equal to load current. This can be seen from t=0 to t=0.1 sec. Figures (9) and (10) show that real and reactive demand of the load is supplied by the grid. The grid current and its THD are shown in figure (11).

Case II: at t=0.1sec, VSI is connected to the system with zero PV power generation. Now the VSI acts in pure APF mode. The reactive power demand of the load is supplied by the inverter as shown in figure (10). Now the grid current is near sinusoidal as clear from figures (8) and figure (12). The corresponding grid, VSI and load active power are shown in figure (9). There is slight increase in the grid active power demand as VSI draws fraction of active power to overcome inverter losses. The grid current and its THD are shown in figure (12) for this mode of operation.

Case III: at t=0.2 sec, the PV system generates power less than load active power demand. Now the grid current is reduced as part of the load current is shared by the PV source. As seen from figure (9), the grid active power is reduced by the same amount to that of the active power generated by the PV system. The remaining KVA capacity of the VSI is used to compensate for the reactive power demand of the load. Part of the reactive power is fed back to the grid due to line inductance.

This result can be seen in figure (10). The grid current remains near sinusoidal.

Case IV: at t=0.3 sec, the PV system generates power more than the load active power demand. The additional active power now is returned to the grid. This is clear from the reverse direction of grid current at this instant. The reactive power requirement is still maintained

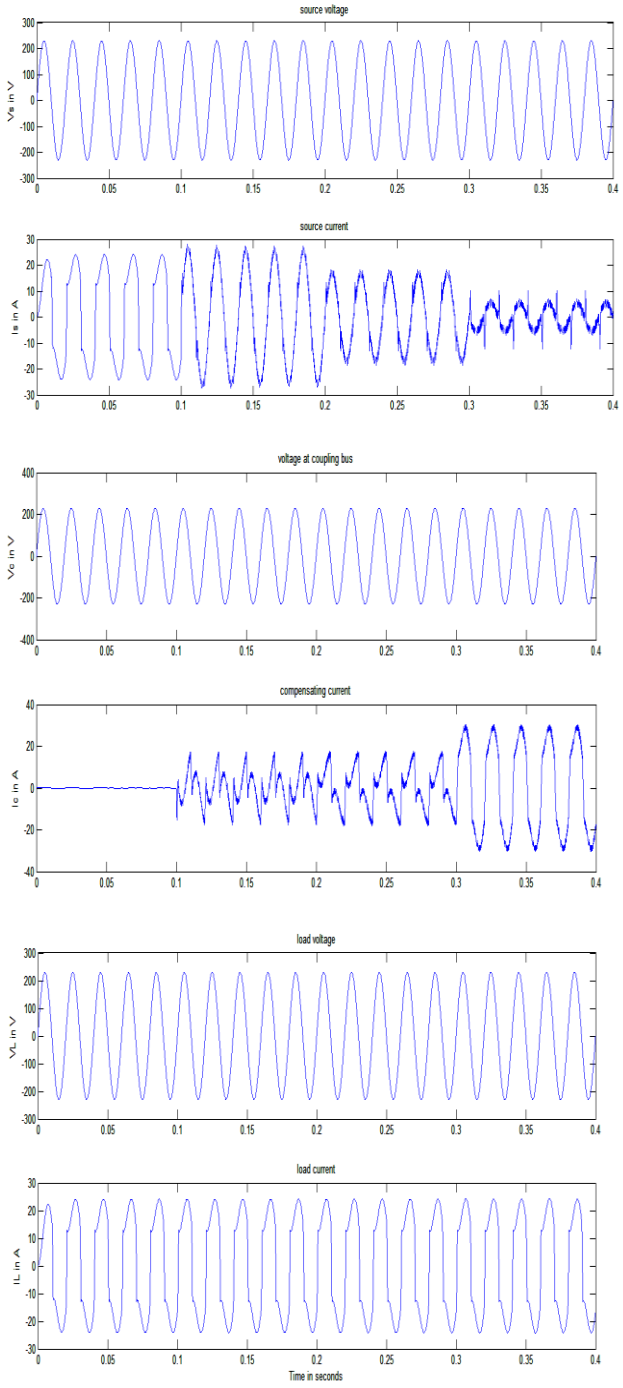

Fig.8. Voltage and currents at different points

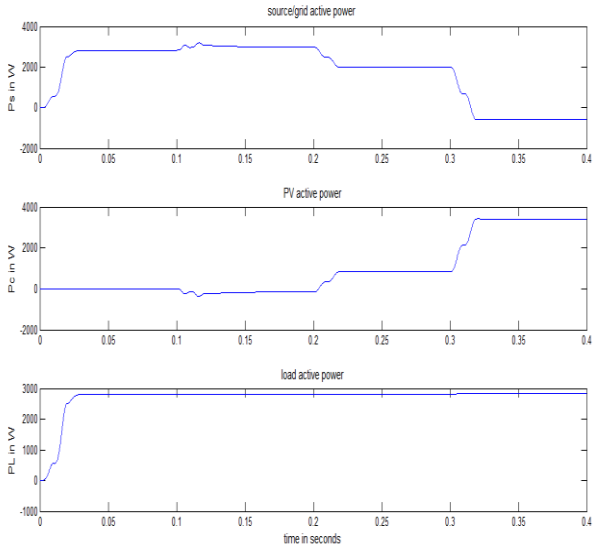

Fig. 9. Active power distribution

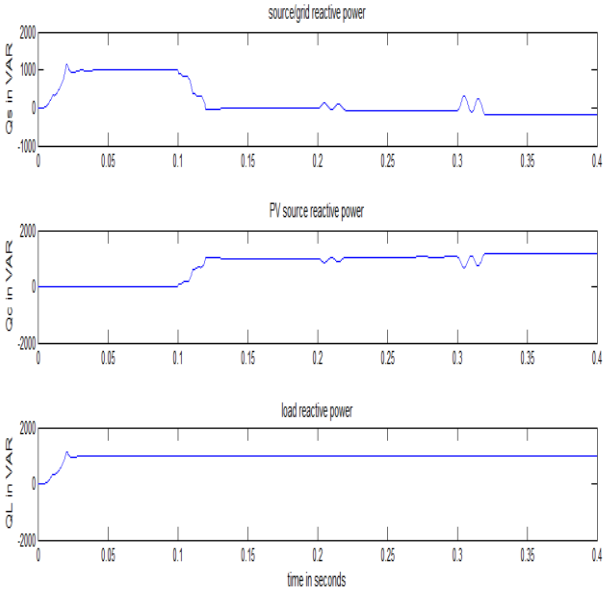

Fig. 10. Reactive power distribution

8. Conclusions

This paper presents the modeling and simulation of a grid connected PV system with APF functionality. The active power supplied by the PV system depending on environmental condition is injected into the grid. The local load active and reactive power is compensated by the PV system.

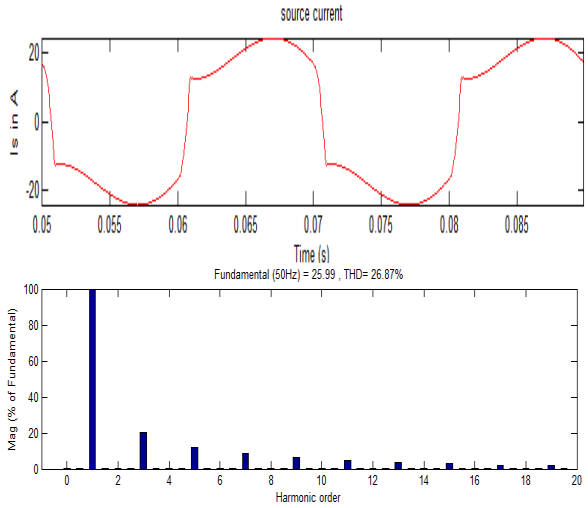

Fig.11. The grid current and its THD without APF

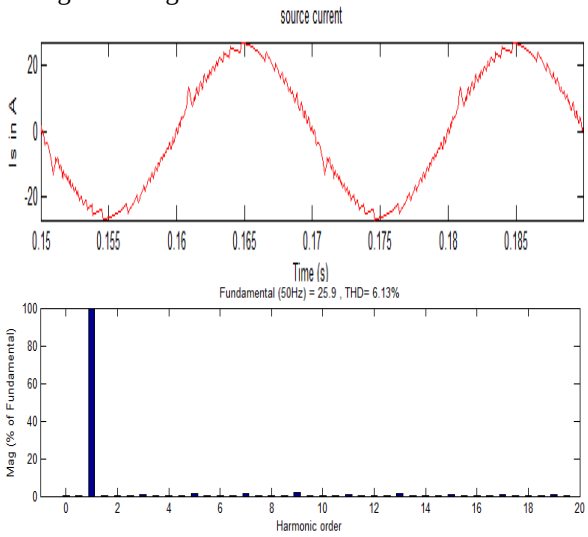

Fig.12. The grid current and its THD with APF

Hence this system behaves as an integration of active power source and APF with minimum hardware (as same VSI is used for real and reactive power injection) and simple control algorithm. The new simple MPPT algorithm is simulated in this paper. After compensation the grid current becomes sinusoidal and in phase with the voltage.

REFERENCES

1. T. E. McDermott and R. C. Dugan," *Distributed generation impact on reliability and power quality indices*" in Proc. IEEE Rural Electr. Power Conf., 2002, pp. D3-D3_7.

2. Y. C. Kuo, T. J. Liang, J. F. Chen, "*Novel maximum-power-point-tracking controller for photovoltaic energy conversion system*," IEEE Trans. on Industrial Electronics, Vol.48 No.3, June 2001, pp. 594-601.

3. J. A. M. Bleijs, J. A. Gow," *Fast maximum power point control of current-fed DC-DC converter for photovoltaic arrays*," Electronics Letters, Vol. 37, N.1, 4 Jan. 2001, pp.5-6.

4. J. A. Gow, C. D. Manning," *Controller management for boost converter systems sourced from solar photovoltaic arrays or other maximum power sources*," IEE Proceedings of Electric Power Applications, Vol.147, No. 1, Jan. 2000, pp.15-20.

5. C . Hua, C. Shen, "*Comparative study of Peak Power Tracking Techniques for Solar Storage Systems",* IEEE Applied Power Electronics Conference and Exposition Proceedings, Vol 2, pp. 679-683, Feb. 1998.

6. R.I. Bojoi, L. R. Limongi, D. Roiu, A. Tenconi," *Enhanced power quality control strategy for single-phas e inverters in distributed generation systems*," IEEE Transaction on Power Electronics, Vol. 26, No. 3, March 2011.

7. Z. Dejia, Z. Zhengming, M. Eltawil, and Y. Liqiang, "*Design and control of a three-phase grid-connected photovoltaic system with developed maximum power tracking*," Applied Power Electron. Conf. and Exposition (APEC), pp. 973-979, 2008.

8. M. E. Ropp and S. Gonzalez, "*Development of a MATLAB/Simulink model of a single-phase Grid-connected photovoltaic system*," IEEE Trans. Energy Convers., vol. 24, no. 1, pp. 195-202, Mar. 2009.

9. L. A. Moran, L. Fernandez, J. W. Dixon, and R. Wallace, "*A Simple and low-cost control strategy for active power filters connected in cascade*," IEEE Trans. Ind. Electron., vol. 44, no. 5, pp. 621-629, Oct. 1997.

10. R. D. Patidar, S. P. Singh, D. K. Rathod," *Single-phase single-stage grid-interactive Photovoltaic system with active filter functions".* IEEE conference on Power and Energy Society General Meeting, 2010.pp. 1-7.

11. E. Koutroulis, K. Kalaitzakis, and N. C. Voulgaris, "*Development of a microcontroller-based photovoltaic MPPT control system*," IEEE TransPower Electron., vol. 16, no. 1, pp. 46-54, Jan. 2001.

12. N. Femia, G. Petrone, G. Spagnuolo, and M. Vitelli, "*Optimization of perturb and observe maximum power point tracking method*," IEEE Trans. Power Electron., vol. 20, no. 4, pp. 963-973, Jul. 2005.

13. M. Buresch: Photovoltaic Energy System Design and Installations, McGraw-Hill, New York, *1983.*

14. Theirry Thomas, Kevork Haddsd, Geza Joos and Alain Jaafari "*Design and performance of active power filters*," IEEE Industry Applications Magazine, pp 38-46 September/October 1998